



Article

Fabrication Temperature-Related Porosity Effects on the Mechanical Properties of Additively Manufactured CFRP Composites

Olusanmi Adeniran ^{1,*}, Norman Osa-uwagboe ^{2,3}, Weilong Cong ¹ and Monsuru Ramoni ⁴

¹ Department of Industrial, Manufacturing, and Systems Engineering, Texas Tech University, Lubbock, TX 79409, USA

² Wolfson School of Mechanical, Electrical, and Manufacturing Engineering, Loughborough University, Loughborough, Leicestershire LE11 3TU, UK

³ Air Force Research and Development Centre, Nigerian Air Force Base, Kaduna PMB 2104, Nigeria

⁴ Department of Industrial Engineering, Navajo Technical University, Crownpoint, NM 87313, USA

* Correspondence: olusanmi.adeniran@ttu.edu; Tel.: +1-(682)-561-4015

Abstract: The use of additive manufacturing in fabricating composite components has been gaining traction in the past decade. However, some issues with mechanical performance still need to be resolved. The issue of material porosity remains a pertinent one which needs more understanding to be able to come up with more viable solutions. Different researchers have examined the subject; however, more research to quantitatively determine fabrication temperatures effects at the micro-scale are still needed. This study employed micro-CT scan analysis to quantitatively compare fabrication temperatures effect at 230 °C, 250 °C, 270 °C, and 290 °C on the mechanical properties of AM fabricated carbon-fiber-reinforced plastic (CFRP) composites, testing carbon fiber-reinforced polyamide (CF-PA) and carbon fiber-reinforced acrylonitrile butadiene styrene (CF-ABS) samples. This micro-CT examination followed an SEM evaluation, which was used to determine temperature effects on interlayer and intralayer porosity generation. The porosity volume was related to the mechanical properties, in which it was determined how temperatures influence porosity volumes. It was also determined that fabrication temperature generally affects semicrystalline composites more than amorphous composites. The overall porosity volumes from the interlayer and intralayer voids were determined, with the interlayer voids being more influential in influencing the mechanical properties.

Keywords: additive manufacturing; fabrication temperature; porosity effects; carbon fiber-reinforced polymer composites; mechanical properties; micro-CT scan; scanning electron microscopy



Citation: Adeniran, O.; Osa-uwagboe, N.; Cong, W.; Ramoni, M. Fabrication Temperature-Related Porosity Effects on the Mechanical Properties of Additively Manufactured CFRP Composites. *J. Compos. Sci.* **2023**, *7*, 12. <https://doi.org/10.3390/jcs7010012>

Academic Editor: Yuan Chen

Received: 11 December 2022

Revised: 22 December 2022

Accepted: 3 January 2023

Published: 5 January 2023



Copyright: © 2023 by the authors. Licensee MDPI, Basel, Switzerland. This article is an open access article distributed under the terms and conditions of the Creative Commons Attribution (CC BY) license (<https://creativecommons.org/licenses/by/4.0/>).

1. Introduction

1.1. Additively Manufactured CFRP Composites

The rapid increase in demand for products with diverse applicability, accuracy, and ease of manufacturing has led to the advancement of flexible manufacturing techniques. In the past two decades, the concept of AM has grown into a reliable method of producing complex structures for several industries, such as aerospace, biomedical, automobile, telecommunications, defense, and renewable energies [1]. These expanding applications can be traced to the advantage of manufacturing prototypes quickly at lower costs and without specialized tooling [2–4].

A distinguishing feature of CFRP composites fabricated by AM is interlayers. These contribute immensely to the degree of porosity in the material, which determines its mechanical performance. The interlayers are characterized by relatively large triangular voids of similar sizes, which are formed by gaps between the print beads during deposition. This often compounds the issue of porosity, resulting in poorer mechanical properties than for parts fabricated through other manufacturing methods. Hence, the importance of a better understanding of fabrication temperature influenced interlayer and intralayer

porosity effects. To advance the manufacturing technique, a greater understanding of the process effect is still needed to improve the viability of the manufacturing method.

1.2. Current Understanding of Deposition Temperature-Related Porosity Effects in AM Fabricated CFRP Composites

Different studies have conducted investigations on porosity effects on the mechanical performance of AM-fabricated CFRP composites [5–12]. However, there have been limited investigations on the quantitative comparison of fabrication temperature-related porosity effects. A better understanding provided by more detailed micro-CT analysis is still needed to cultivate knowledge of how deposition temperatures influence porosity features and affect the mechanical performance of AM-fabricated CFRP composites. The investigations that examined porosity effects did not evaluate deposition temperature effects, and those that examined temperature effects did not qualitatively compare porosity effects.

Zhang et al. [5] examined interlayer porosities as influenced by printing raster angles in AM-fabricated CFRP composites but did not consider the effects of deposition temperatures. Petro et al. [9] explored an X-ray CT scan to determine porosity volumes in a 41% fiber content continuous CFRP composite, where they compared the results to the ASTM D3171 standard. However, they did not consider fabrication temperature-related porosity effects. Tekinalp et al. [6] investigated the effect of fiber volumes on tensile properties and the degree of porosity. However, they did not examine the effect of printing temperatures or provide a clear measurement procedure to arrive at their reported porosity values. Ning et al. provided porosity measurements in two of their reported investigations [7,13] that examined the effects of fiber content and the effects of reinforcement materials on porosities. However, they applied a rudimentary measurement procedure, where they performed manual weighing of samples and subtraction from a calculated solid mass. In another study [14] where the authors tested the effects of process factors including fabrication temperatures, they did not measure or compare porosity volumes.

Other reported investigations on the effects of process temperatures on the mechanical performance of AM-fabricated CFRP composites have been devoted to layer strength from matrix material viscoelasticity fluidity rather than addressing the topic of temperature-related porosity effects [15–19]. Ajinjeru et al. [15] investigated the viscoelasticity of polyetherimide (PEI) matrix at different process temperatures to gain more understanding of the effects of matrix material fluidity on the ease of processing but did not examine porosity effects. These researchers also investigated acrylonitrile butadiene styrene (ABS) and polyphenyl sulfone (PPSU) to determine suitable processing conditions [16], but also did not investigate porosity. Kishore et al. [17] investigated interlayer strength improvement by using infrared heating to increase the surface temperature of the printed layer just before the deposition of the succeeding layer, thus improving surface properties; however, they did not examine temperature-influenced porosity. Yang et al. [19] investigated a novel process consisting of continuous fiber hot-dipping, matrix material melting, and impregnated composite extrusion to improve composite properties, but did not discuss the topic of temperature-related porosity effects.

1.3. Research Motivation

Of all the known challenges to the successful application of AM-fabricated CFRP composites, the issue of interlayer and intralayer porosity is one of the most pertinent, requiring better understanding. However, a detailed quantitative understanding of the effect of printing temperature-influenced porosity on the mechanical performance of the composites is not well developed. This motivated our study to investigate the effects of printing temperature-related porosity on the mechanical performance of the composite for samples fabricated using the fused deposition modeling (FDM) technique. The investigations included evaluating the relationships between printing temperatures, mesostructure formation, fabrication porosities, and the mechanical properties of the composite. The

understanding gained contributes to knowledge of fabrication temperature process control for the improved mechanical performance of CFRP composites fabricated by AM.

2. Materials and Methods

2.1. AM Workpiece Fabrication Procedure

Test workpieces used to conduct the investigations were fabricated from two different CFRP composite materials with manufactured carbon fibers with an average diameter of 7 μm and length of less than 400 μm : 15% CF-PA6 filament compounded from high-modulus short carbon fiber in a PA6 copolymer (3D XTEC, Grand Rapids, MI, USA) and 15% CF-ABS filament compounded from high-modulus short carbon fiber in Sabcic MG-94 ABS (3D XTEC, Grand Rapids, MI, USA).

A 3D printer (Prusa Mk3 i3, Prague, Czech Republic) was used for the FDM fabrication in a modified control printing enclosure fixture (Creality 3D, Shenzhen, China) to maintain a 45 ± 5 °C printing environment temperature and relative humidity of lower than 20% RH. The 230 °C–290 °C printing temperature range was chosen to determine how fabrication temperatures influence porosity volume because of the material viscosities and flowability within that temperature range. Table 1 shows the printing parameters used to fabricate the test workpieces and Figure 1 illustrates the 3D printer setup employed.

Table 1. Material processing parameters.

Parameter	Unit	Value
Infill Density	%	100
Printer Enclosed Temperature	°C	50 ± 5
Bed Temperature	°C	100
Raster Angle	Deg	0, 90
Layer Thickness	mm	0.25
Printing Speed	mm/sec	30
Nozzle Temperature	°C	230, 250, 270, 290

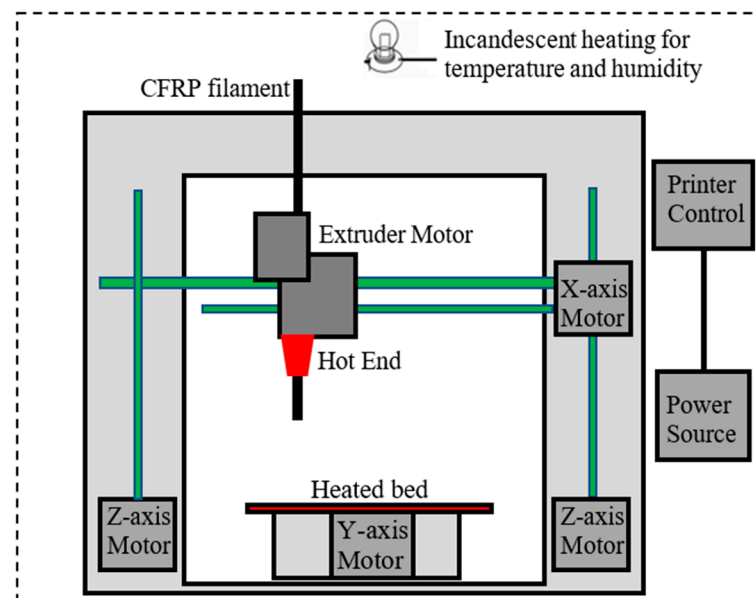


Figure 1. Setup of a 3D printer to control immediate printing environment temperature and humidity. Based on Adeniran et al. [20].

2.2. Measurement Procedure

2.2.1. Mechanical Measurements

Tensile samples that consisted of four workpieces per data point for the AM-fabricated CF-PA and CF-ABS composites were tested to quantitatively compare fabricating temperature-

related porosities and the resulting effects on the mechanical properties of the composites. A 10 kN load cell in a universal mechanical tester (MTS Criterion Model 45, Eden Prairie, MN, USA) was used to conduct tensile tests, while a 10 kg minor load and a 100 kg major load were used in the Rockwell tester (Clark C12A, Novi, MI, USA) to conduct the hardness test. Table 2 shows the test procedures applied in the study.

Table 2. Test standards and equipment.

Test	ASTM Standard	Equipment	Test Speed	Unit
Tensile	D638 (Type I)	MTS Criterion Model 45	5.0	mm/min
Rockwell Hardness	D785	Clark Tester C12A	-	-
Scanning Electron Microscopy	-	Thermo Scientific Phenom XL	100×	Magnification
Micro-CT	-	Nikon X-Tex XTH	2	Proj/sec

2.2.2. Scanning Electron Microscopy

Cross-sections of fractured tensile workpieces of the CF-PA and CF-ABS composite samples printed at 230 °C, 250 °C, 270 °C, and 290 °C were examined at 100× magnification in a scanning electron microscope (Thermo Fisher Phenom XL, Waltham, MA, USA) to evaluate the mesostructure formation of the composites as determined by the deposition temperature and matrix materials.

2.2.3. Micro-CT Microscopy

To improve the accuracy of the temperature influenced-porosity determination, 3 samples, each with cross-section volumes of 25 mm × 9 mm × 2.5 mm, were scanned for each data point of the 230 °C, 250 °C, 270 °C, and 290 °C composite samples. Each cross-sectional volume was divided into 6 segments (1A–3B), as illustrated in Figure 2, with the average mean porosity values determined over the segmented volumes while Figure 3 shows the micro CT microscope (Nikon XTH X-TeX 160Xi, France) configuration used for the measurement.

The scan was performed on the CT scan microscope with the scanning point-to-point resolution set to 2.5 μm at an exposure time of 500 ms with a total of 3016 tiff images created per sample scan. The acquired microscopy data were transferred and post-processed using commercial software (Dragonfly ORS, Adelaide, South Australia, Australia). The automatic features of the software were used to determine the optimum center of rotation, with all generated slices combined to develop the volumetric image in the reconstruction phase. Characterization noise generated with the volumetric imaging was reduced using Gaussian filters, which, in the case of this investigation, resulted in minimal data loss from the sample materials' homogeneity. The generated tiff files were incorporated into the software with voxel analysis to determine volumetric porosity.

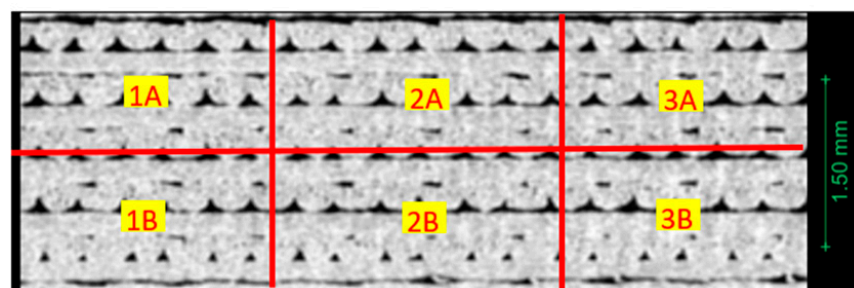


Figure 2. Illustration of segmented volume areas used in micro-CT porosity determination of AM-fabricated CFRP composites.

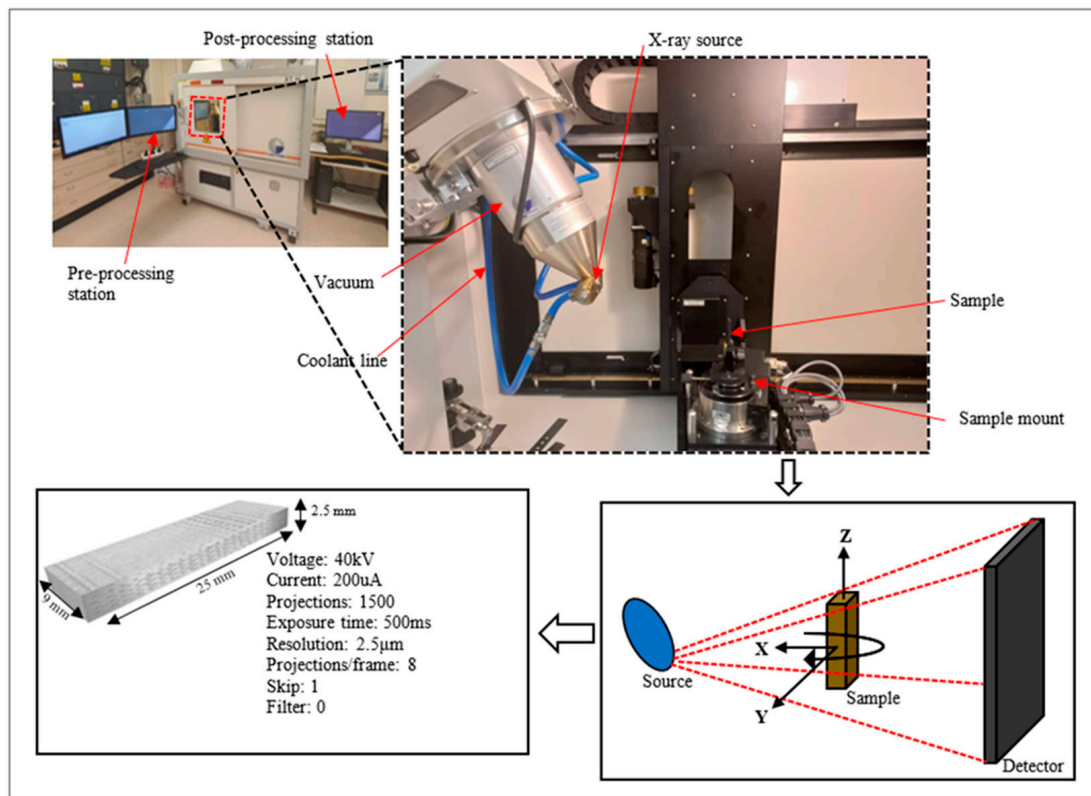


Figure 3. X-ray micro-CT setup and detailed scanning parameters.

3. Results

3.1. Scanning Electron Microscopy Results

SEM determination was used to interpret the effects of printing temperatures of 230 °C to 290 °C on interlayer and intralayer porosity generation for the composites. The thermal history of adjoining melt layers as determined by deposition temperatures influences the extrusion melt solidification, bonding, and the interlayer feature formed including the degree of porosity.

3.1.1. SEM Result for CF-PA Composite

Figure 4 shows the SEM observations of the mesostructure features for the AM-fabricated CF-PA composites.

The SEM examination of the AM-fabricated CF-PA composite shows increasing fiber matrix coalescence with nozzle head temperature for the 230 °C–290 °C temperature range examined. A spongy-like mesostructure with less regular layer formation was observed, which can be attributed to the excessive shrinkage of the semicrystalline matrix recrystallization on cooling from fabrication. The low melt viscosity of the semicrystalline morphology can also be ascribed to contribute to the irregular interlayer mesostructure formation. According to Vaes and Puyvelde [21], porosities could be an issue in semicrystalline matrix AM fabrication due to the heterogenous self-nucleation of their structural crystals from insufficient heat transfer, melting, and high shear deformations during fabrication to influence the material's porosities.

The fusion bonding theory applies to AM composite fabrication, where the increasing heat from the 230 °C–90 °C nozzle head temperatures in this case improved the carbon fiber matrix coalescence to reduce interlayer porosities. This is because the higher the fabrication temperature is above the glass transition temperature, the more even the mechanisms of chain rearrangement in the print are during the heating and solidification processes [22].

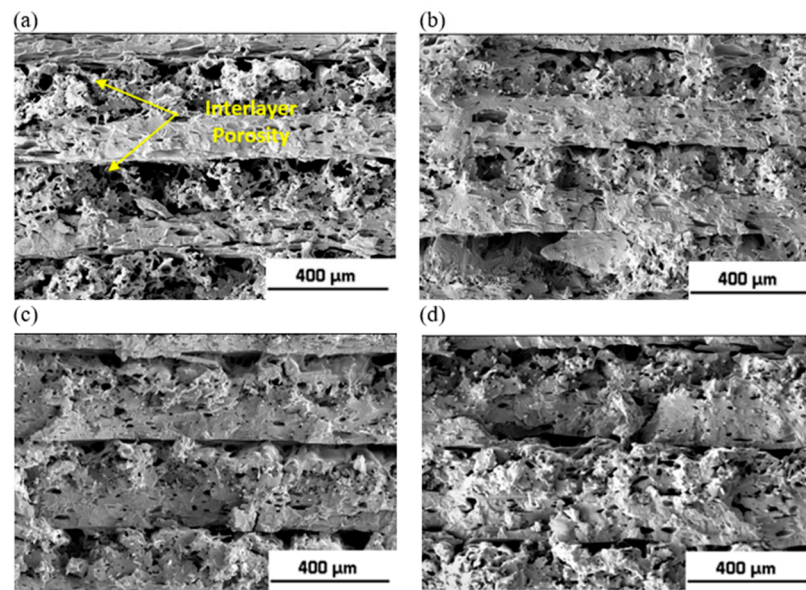


Figure 4. Mesostructure of CF-PA composites printed at (a) 230 °C, (b) 250 °C, (c) 270 °C, (d) 290 °C [100×].

3.1.2. SEM Result for CF-ABS Composite

Figure 5 shows the SEM observation of the mesostructure features for the AM-fabricated CF-ABS composites.

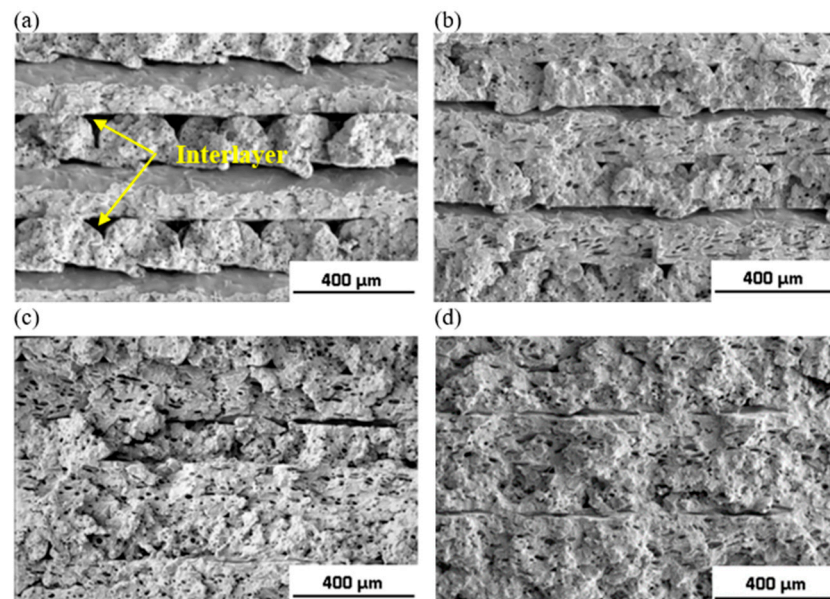


Figure 5. Mesostructure of CF-ABS composites printed at (a) 230 °C, (b) 250 °C, (c) 270 °C, (d) 290 °C [100×].

The SEM evaluation in Figure 5 shows that the CF-ABS composite exhibits a regular arrangement of the interlayers in the mesostructure. This is because of the high fluidity of the ABS matrix during solidification [23]. Increasing the fabrication temperatures between 270 °C–290 °C showed improved mesostructure formation and reduced interlayer porosities that were attributable to the improved melt flow at the increased temperatures. However, the steeper temperature gradient on cooling due to the higher temperatures resulted in greater intralayer porosity.

Similar to Figure 4, plastic material fusion bonding theory can also be applied to explain how increased heating from nozzle head temperatures can improve carbon fiber

matrix coalescence and reduce interlayer porosities in the CF-ABS composites. However, at more elevated temperatures, temperature increases become detrimental and may result in degraded molecular chain strength, resulting in reduced mechanical performance, as was seen for the composite at the 290 °C fabrication temperature.

3.2. Micro-CT Scan Result

The micro-CT scan provides a more detailed quantitative evaluation of porosity features. Through the scan, porosity volume comparisons for the different fabrication temperatures were determined. Figure 6 presents reconstructed CT scan void images for the CF-PA and CF-ABS composites, which show a general void reduction with the increasing fabrication temperature under study.

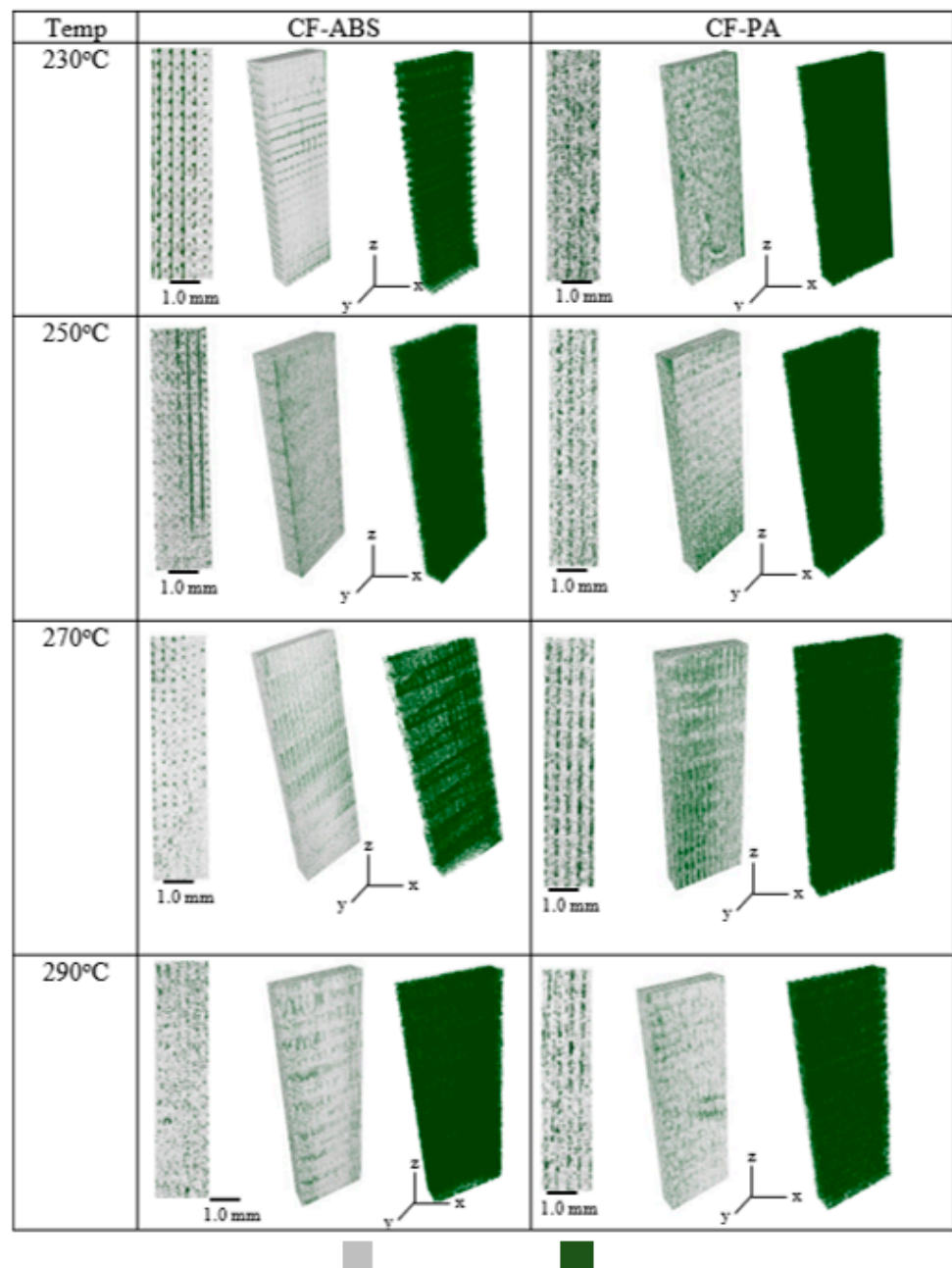


Figure 6. Reconstructed X-ray CT void for CF-ABS and CF-PA composite specimens for the different fabrication temperatures under study.

The variation is visualized with the grey pixels representing the solid volume of the composite and the green pixels representing the porosities. Understanding the effects of fabrication temperature on the degree of porosity is vital to characterizing the composites' mechanical performance to gain insights into how they affect material properties such as strength, modulus, ductility, toughness, hardness, etc. This is needed to determine the range of fabrication temperatures required to achieve the required material properties for different applications. Figures 7 and 8 show a plot of the test results for the CF-PA and CF-ABS composites, respectively, fabricated between 230 °C and 290 °C.

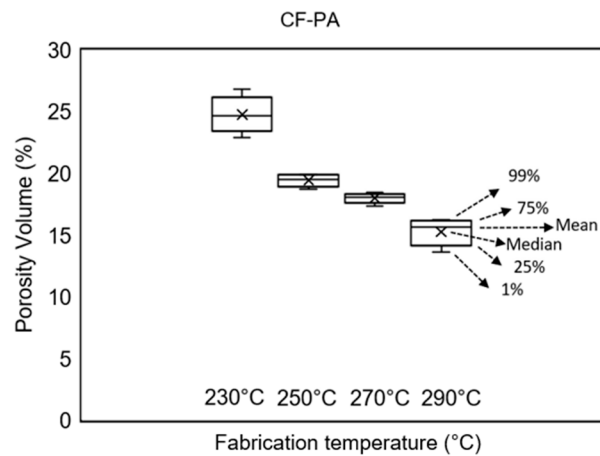


Figure 7. Fabrication temperature-related porosity volume in AM-fabricated CF-PA composite.

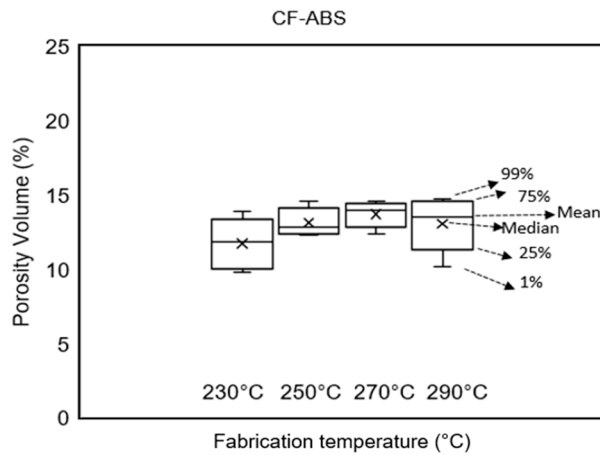


Figure 8. Fabrication temperature-influenced porosity volume in AM-fabricated CF-ABS composite.

3.2.1. Micro-CT Scan Porosity Results for CF-PA Composite

The results show an overall trend of reduced porosity from the combined inter and intra-layer porosities effect when increasing the fabrication temperature from 230 °C to 290 °C.

Figure 7 shows a gradual decrease in the porosity of the CF-PA composite as the fabrication temperature increased from 230 °C to 290 °C, with a plot of test data distribution in percentiles within the overall data set. The composites show a consistent reduction in porosity volumes with mean values of 24.7%, 19.4%, 18.0%, and 15.3% for 230 °C, 250 °C, 270 °C, and 290 °C, respectively. A reduced porosity was observed with increasing temperature due to the fiber matrix's increasing coalescence, resulting in more solid mesostructure formation with reduced interlayer features.

3.2.2. Micro-CT Scan Porosity Results for CF-ABS Composite

Figure 8 shows the results for the overall porosity trends for CF-ABS within the 230 °C to 290 °C fabrication temperature range under study.

Even though the SEM evaluations of the composite showed pronounced interlayer porosity differences with fabrication temperature, the effect on the overall porosity volume for the amorphous CF-ABS was not quite pronounced when quantitatively measured in the CT scan. Figure 8 shows the overall porosity volume differences were insignificant with mean values of 11.7% for the 230 °C, 13.1% for the 250 °C, 13.9% for the 270 °C, and 13.1% for the 290 °C samples. Increasing the deposition temperature from 230 °C to 290 °C resulted in more interlayer coalescence with reduced interlayer porosities. However, intralayer porosities increased as a result of the steeper temperature gradient on cooling. These overall effects from the inter and intra layers were seen to account for the cause of the insignificant differences in the porosity volumes observed across the 230 °C to 290 °C deposition temperature range. The study by Adeniran et al. [24] provided more insight into the porosity types generated in CF-ABS composites fabricated by AM, where they discussed two fabrication-generated porosity types. The interlayer porosities are explained as triangular gaps in the non-contact areas of the print beads during layer-upon-layer material build-up while intralayer porosities are the void formation inside individual print beads due to gas evolution in the course of the semi-liquid to extrusion of the print material.

3.3. Fabrication Temperature-Related Porosity Effects on Mechanical Properties

3.3.1. Mechanical Properties of CF-PA Composite

A generally significant effect of fabrication temperature-influenced porosity effects within a 230 °C to 290 °C range on the tensile performance of AM-fabricated CF-PA composite was observed. This is in line with the CT scan microscopy results in Section 3.2.1, which showed the overall porosity reduced by as much as 38% from 230 °C to 290 °C for the samples investigated. Figure 9 shows the different mechanical properties examined for the AM-fabricated CF-PA composite.

Tensile Strength: The material tensile strength shown in Figure 9a is an indication of the maximum stress that can be applied while stretched in tension before material failure by elastic or plastic deformation. Printing temperatures played some role in influencing tensile strength, which may be related to the interlayer porosity feature as shown by the mesostructure formation and micro-CT scan evaluation in Sections 3.1.1 and 3.2.1, respectively. A significant effect was observed for the fabricated CF-PA composite, which displayed up to 37% increase in tensile strength at an optimized 290 °C printing temperature compared to the 230 °C baseline.

Fabrication temperature effects can be explained with better fiber matrix and layer-to-layer molecular bonding at higher temperatures, which promotes better inter-laminar and cross-laminar chemical bonding between print layers. This follows the explanation by Brenken et al. [25] that fabrication temperatures have strong effects on the melt viscosity of plastic matrices for bond formation between adjacent layers. Higher temperatures further from the glass transition temperature promote the diffusion-based fusion of adjacent layers after interfaces are established, while lower temperatures usually result in decreased molecular mobility, which hinders the molecular diffusion process.

Tensile Modulus: The modulus values define the stiffness properties of the material. As seen in Figure 9b, fabrication temperatures have insignificant effects on the CF-PA composite. Less than 10% variation was observed in the modulus properties for the 230 °C to 290 °C print temperature range. The insignificant effects of fabrication temperature can be explained by the theory propounded by Vaes and Puyvelde [21], which explained the effect of temperature in determining material modulus. They discussed modulus as influenced by the heterogenous self-nucleation of the structural crystals of the composite, which are influenced by heat transfer, melting, and shear deformations during the fabrication process. However, no great effect was observed for the 230 °C to 290 °C temperature range examined.

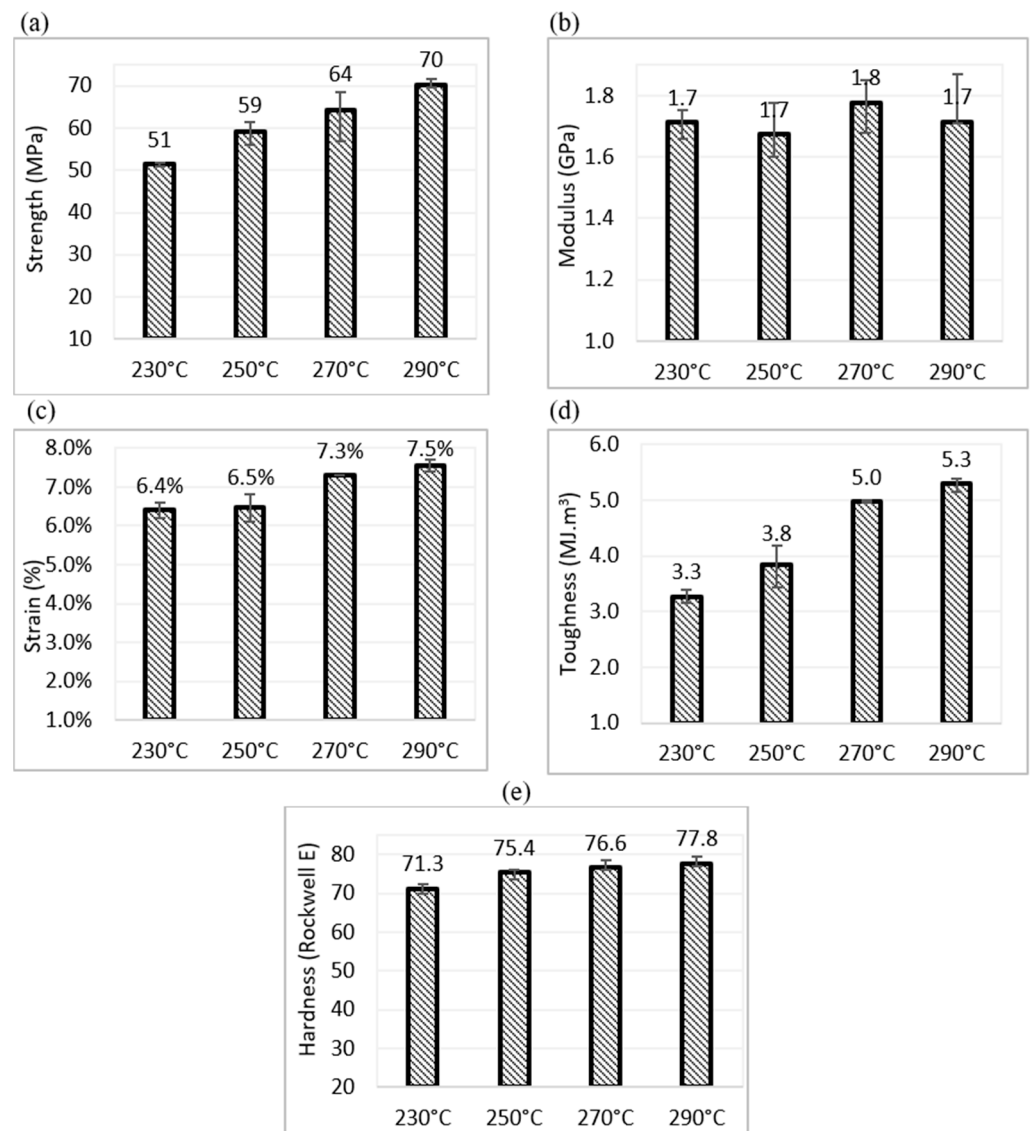


Figure 9. Tensile properties of semi-crystalline CF-PA composites at different printing temperatures: (a) ultimate tensile strength, (b) modulus, (c) ductility, (d) toughness, (e) hardness.

Tensile Ductility: The property of ductility measures the material's characteristics for plastic deformation before fracture. The results in Figure 9c show fabricating temperature trends similar to those observed for tensile strength in Figure 9a. Up to a 17% increase in ductility properties was observed at the 290 °C fabrication temperature, which offered the optimal temperature compared to the 230 °C temperature. The reduced degree of porosity volumes with increasing fabrication temperatures can be used to explain this increase in ductility with temperature when the materials are subjected to strain.

Tensile Toughness: The composite material's ability to absorb energy and plastically deform without fracturing is provided by its toughness values. As seen in Figure 9d, similar to the strength and ductility properties, fabrication temperature has some significant effects on the toughness properties of the CF-PA composite, with an approximate 60% increase in value observed at the highest 290 °C temperature over the 230 °C baseline. The toughness property, generally determined by the material strength and ductility characteristics, has similar determining features to the material strength and ductility, which also influence the toughness property.

Hardness: The Rockwell hardness number directly relates to the indentation hardness of the material and defines the resistance of a material to localized plastic deformation.

Figure 9e shows the Rockwell E values for the CF-PA composite exhibiting similar deposition temperatures related to hardness trends as the other mechanical properties. Although not as significant as the other properties, there was an upward increase in value with increasing deposition temperatures from 230 °C to 290 °C, which may also be related to the decreased porosities with increasing fabrication temperatures up to 290 °C.

3.3.2. Mechanical Properties of CF-ABS Composite

A generally insignificant effect of fabrication temperature-influenced porosity within a 230 °C to 290 °C range was observed on the tensile performance of AM-fabricated CF-ABS composite. This is in line with the CT scan microscopy results in Section 3.2.2, which showed the overall porosity for the most part to be within the range of 15%, except for the 270 °C fabricating temperature that showed a deviated range of up to 43% from the three other temperature data points under examination. Figure 10 shows the different mechanical properties examined for the CF-ABS composite.

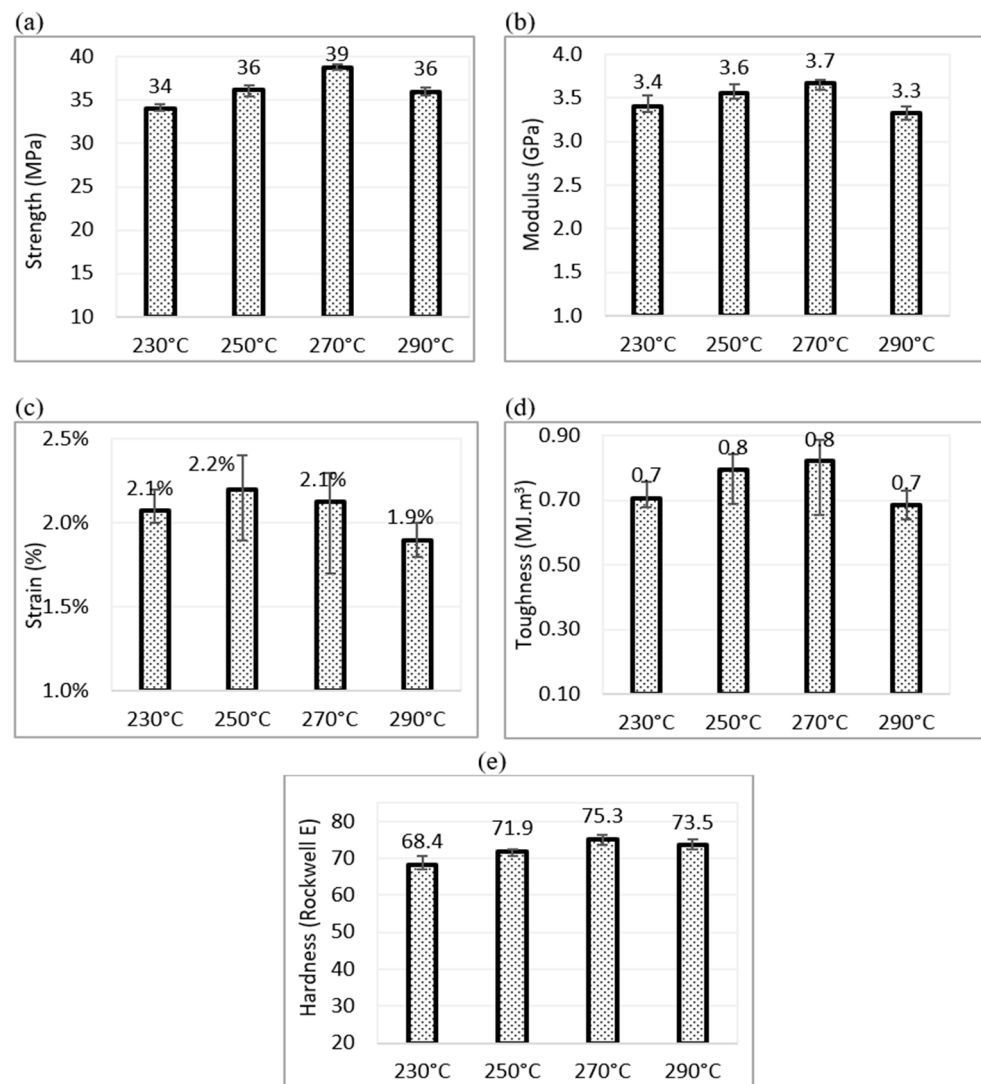


Figure 10. Tensile properties of amorphous CF-ABS composite at different printing temperatures: (a) ultimate tensile strength, (b) modulus, (c) ductility, (d) toughness, (e) hardness.

Tensile Strength: As seen in Figure 10a, fabrication temperature played some role in influencing the tensile strength of the CF-ABS composite. However, not so significant. An up to 15% increase in strength was observed at 270 °C, which was found to be optimal for the fabrication temperature range under examination.

Similar to the CF-PA composite, the temperature effects can be explained by the theory of better fiber matrix and layer-to-layer molecular bonding with higher printing temperatures, due to their promotion of good inter-laminar and cross-laminar chemical bonding between print layers. This similarly follows the explanation by Brenken et al. [25] that fabrication temperatures strongly influence the melt viscosity of plastic matrices for bond formation between interlayers. High temperatures are needed for the fusion bonding of adjacent beads following interface formation, while lower temperatures usually decrease molecular mobility and limit the molecular diffusion process. However, excessive temperatures can also be detrimental, leading to alteration of the material composition and degradation of the material strength as seen with the CF-ABS composite beyond 270 °C fabrication temperature.

Tensile Modulus: As seen with the tensile strength results for the AM-fabricated CF-ABS composite, fabricating temperature has insignificant effects. Figure 10b shows less than 10% variation for the 230 °C to 290 °C fabrication temperatures examined. The insignificant effect on the tensile modulus can be ascribed to the similarity of overall porosity volumes observed from the CT scan results, which are determinant to the stiffness features that determine the modulus properties of the composite.

Tensile Ductility: As observed for the other tensile properties of the AM-fabricated CF-ABS composite, the material ductility shown in Figure 10c has similar trends for the effect of fabrication temperature. The effects were found to be insignificant within a 10% range for the 230 °C to 290 °C fabrication temperatures examined, which can also be attributed to the insubstantial differences in the overall porosities generated at the different fabrication temperatures.

Tensile Toughness: Figure 10d shows the material toughness, which exhibits similar trends in strength and ductility. Fabrication temperature has an insignificant effect on AM-fabricated CF-ABS composite (less than 10%), with the material strength and ductility properties also known to have an overall effect on this property and similar intrinsic material features that determine strength and ductility also determining the material toughness characteristics.

Hardness Properties: Similar to the tensile strength, ductility, and toughness, the hardness properties for the AM-fabricated CF-ABS composite as seen in Figure 10a show the Rockwell E values, which exhibit similar deposition temperature-related hardness trends. The effect was insignificant but still shows the property value peaking at 270 °C as seen for the other tensile properties. The insignificant differences can also be attributed to the insubstantial effects of the deposition temperature on the overall interlayer and intralayer porosity volume differences for the 230 °C to 290 °C deposition temperatures examined.

4. Conclusions

In this study, deposition temperature-related porosity effects on mechanical properties—strength, modulus, ductility, toughness, and hardness—of AM-fabricated CFRP composites using semicrystalline CF-PA and amorphous CF-ABS samples were examined. The investigations were conducted by relating deposition temperature trends to mesostructure formation, porosities, and mechanical properties, and the following conclusions were drawn:

- (1) Deposition temperatures have some effects on porosity volumes in AM-fabricated CFRP composites, with semicrystalline CF-PA much more significantly affected than the amorphous CF-ABS composite.
- (2) The degree of porosity is largely determined by the characteristics of the matrix material.
- (3) A direct relationship exists between CFRP composites' porosity and mechanical properties.
- (4) The overall porosity volumes are determinant of the interlayer and intralayer voids, but the interlayer voids play a greater role in determining the mechanical properties.
- (5) Semicrystalline composites exhibit higher porosity volumes than amorphous composites due to rapid recrystallization as the chains rearrange during the cooling of the print beads.

Author Contributions: Conceptualization, O.A.; methodology, O.A. and N.O.-u.; validation, O.A.; formal analysis, O.A. and N.O.-u.; investigation, O.A. and N.O.-u.; resources, O.A., M.R. and W.C.; data curation, O.A. and N.O.-u.; writing—original draft preparation, O.A.; writing—review and editing, O.A., M.R. and W.C.; supervision, W.C. All authors have read and agreed to the published version of the manuscript.

Funding: This research received no external funding.

Data Availability Statement: Data used in this research are available upon request in Microsoft txt, Docx, and jpg file formats.

Conflicts of Interest: The authors declare that there is no conflict of interest.

References

1. Frketic, J.; Dickens, T.; Ramakrishnan, S. Automated Manufacturing and Processing of Fiber-Reinforced Polymer (FRP) Composites: An Additive Review of Contemporary and Modern Techniques for Advanced Materials Manufacturing. *Addit. Manuf.* **2017**, *14*, 69–86. [[CrossRef](#)]
2. Melchels, F.P.W.; Feijen, J.; Grijpma, D.W. A Review on Stereolithography and Its Applications in Biomedical Engineering. *Biomaterials* **2010**, *31*, 6121–6130. [[CrossRef](#)]
3. Dimas, L.S.; Buehler, M.J. Modeling and Additive Manufacturing of Bio-Inspired Composites with Tunable Fracture Mechanical Properties. *Soft Matter* **2014**, *10*, 4436–4442. [[CrossRef](#)]
4. Mazzoli, A. Selective Laser Sintering in Biomedical Engineering. *Med. Biol. Eng. Comput.* **2013**, *51*, 245–256. [[CrossRef](#)]
5. Zhang, W.; Cotton, C.; Sun, J.; Heider, D.; Gu, B.; Sun, B.; Chou, T.W. Interfacial Bonding Strength of Short Carbon Fiber/Acrylonitrile-Butadiene-Styrene Composites Fabricated by Fused Deposition Modeling. *Compos. Part B Eng.* **2018**, *137*, 51–59. [[CrossRef](#)]
6. Tekinalp, H.L.; Kunc, V.; Velez-Garcia, G.M.; Duty, C.E.; Love, L.J.; Naskar, A.K.; Blue, C.A.; Ozcan, S. Highly Oriented Carbon Fiber-Polymer Composites via Additive Manufacturing. *Compos. Sci. Technol.* **2014**, *105*, 144–150. [[CrossRef](#)]
7. Ning, F.; Cong, W.; Qiu, J.; Wei, J.; Wang, S. Additive Manufacturing of Carbon Fiber Reinforced Thermoplastic Composites Using Fused Deposition Modeling. *Compos. Part B Eng.* **2015**, *80*, 369–378. [[CrossRef](#)]
8. Adeniran, O.; Cong, W.; Bediako, E.; Aladesanmi, V. Additive Manufacturing of Carbon Fiber Reinforced Plastic Composites: The Effect of Fiber Content on Compressive Properties. *J. Compos. Sci.* **2021**, *5*, 325. [[CrossRef](#)]
9. Petrò, S.; Reina, C.; Moroni, G. X-Ray CT-Based Defect Evaluation of Continuous CFRP Additive Manufacturing. *J. Nondestr. Eval.* **2021**, *40*, 7. [[CrossRef](#)]
10. Tagscherer, N.; Schromm, T.; Drechsler, K. Foundational Investigation on the Characterization of Porosity and Fiber Orientation Using XCT in Large-Scale Extrusion Additive Manufacturing. *Materials* **2022**, *15*, 2290. [[CrossRef](#)] [[PubMed](#)]
11. Adeniran, O.; Cong, W.; Aremu, A.; Oluwole, O. Forces in Mechanics Finite Element Model of Fiber Volume Effect on the Mechanical Performance of Additively Manufactured Carbon Fiber Reinforced Plastic Composites. *Forces Mech.* **2023**, *10*, 100160. [[CrossRef](#)]
12. Adeniran, O. Mechanical Performance of Carbon Fiber Reinforced Plastic Composites Fabricated by Additive Manufacturing. Ph.D. Thesis, Texas Tech University, Lubbock, TX, USA, 2022.
13. Ning, F.; Cong, W.; Hu, Z.; Huang, K. Additive Manufacturing of Thermoplastic Matrix Composites Using Fused Deposition Modeling: A Comparison of Two Reinforcements. *J. Compos. Mater.* **2017**, *51*, 3733–3742. [[CrossRef](#)]
14. Ning, F.; Cong, W.; Hu, Y.; Wang, H. Additive Manufacturing of Carbon Fiber-Reinforced Plastic Composites Using Fused Deposition Modeling: Effects of Process Parameters on Tensile Properties. *J. Compos. Mater.* **2017**, *51*, 451–462. [[CrossRef](#)]
15. Ajinjeru, C.; Kishore, V.; Lindahl, J.; Sudbury, Z.; Hassen, A.A.; Post, B.; Love, L.; Kunc, V.; Duty, C. The Influence of Dynamic Rheological Properties on Carbon Fiber-Reinforced Polyetherimide for Large-Scale Extrusion-Based Additive Manufacturing. *Int. J. Adv. Manuf. Technol.* **2018**, *99*, 411–418. [[CrossRef](#)]
16. Ajinjeru, C.; Kishore, V.; Liu, P.; Lindahl, J.; Hassen, A.A.; Kunc, V.; Post, B.; Love, L.; Duty, C. Determination of Melt Processing Conditions for High-Performance Amorphous Thermoplastics for Large Format Additive Manufacturing. *Addit. Manuf.* **2018**, *21*, 125–132. [[CrossRef](#)]
17. Kishore, V.; Ajinjeru, C.; Nycz, A.; Post, B.; Lindahl, J.; Kunc, V.; Duty, C. Infrared Preheating to Improve Interlayer Strength of Big Area Additive Manufacturing (BAAM) Components. *Addit. Manuf.* **2017**, *14*, 7–12. [[CrossRef](#)]
18. Cinquin, J.; Chabert, B.; Chauchard, J.; Morel, E.; Trotignon, J.P. Characterization of a Thermoplastic (Polyamide 66) Reinforced with Unidirectional Glass Fibres. Matrix Additives and Fibres Surface Treatment Influence on the Mechanical and Viscoelastic Properties. *Composites* **1990**, *21*, 141–147. [[CrossRef](#)]
19. Yang, C.; Tian, X.; Liu, T.; Cao, Y.; Li, D. 3D Printing for Continuous Fiber Reinforced Thermoplastic Composites: Mechanism and Performance. *Rapid Prototyp. J.* **2017**, *23*, 209–215. [[CrossRef](#)]
20. Adeniran, O.; Cong, W.; Aremu, A. Material Design Factors in the Additive Manufacturing of Short Carbon Fiber Reinforced Plastic Composites: A State-of-the-Art-Review. *Adv. Ind. Manuf. Eng.* **2022**, *5*, 100100. [[CrossRef](#)]

21. Vaes, D.; van Puyvelde, P. Semi-Crystalline Feedstock for Filament-Based 3D Printing of Polymers. *Prog. Polym. Sci.* **2021**, *118*, 101411. [[CrossRef](#)]
22. Jiang, Z.; Diggle, B.; Tan, M.L.; Viktorova, J.; Bennett, C.W.; Connal, L.A. Extrusion 3D Printing of Polymeric Materials with Advanced Properties. *Adv. Sci.* **2020**, *7*, 1–32. [[CrossRef](#)] [[PubMed](#)]
23. Gofman, I.v.; Yudin, V.E.; Orell, O.; Vuorinen, J.; Grigoriev, A.Y.; Svetlichnyi, V.M. Influence of the Degree of Crystallinity on the Mechanical and Tribological Properties of High-Performance Thermoplastics over a Wide Range of Temperatures: From Room Temperature up to 250 °C. *J. Macromol. Sci. Part B Phys.* **2013**, *52*, 1848–1860. [[CrossRef](#)]
24. Adeniran, O.; Cong, W.; Bediako, E.; Adu, S.P. Environmental Affected Mechanical Performance of Additively Manufactured Carbon Fiber-Reinforced Plastic Composites. *J. Compos. Mater.* **2022**, *56*, 1139–1150. [[CrossRef](#)]
25. Brenken, B.; Dissertation, A. Extrusion Deposition Additive Manufacturing of Fiber Reinforced Semi-Crystalline Polymers. Ph.D. Thesis, Purdue University, West Lafayette, IN, USA, 2017.

Disclaimer/Publisher’s Note: The statements, opinions and data contained in all publications are solely those of the individual author(s) and contributor(s) and not of MDPI and/or the editor(s). MDPI and/or the editor(s) disclaim responsibility for any injury to people or property resulting from any ideas, methods, instructions or products referred to in the content.